Electronic Supplementary Material (ESI) for Environmental Science: Nano.


# Supporting information

## An upcycled wood sponge adsorbent for drinking water purification by solar steam generation

**Meng Li[1,*], Mengwen Xu[1], Quanyu Shi[1], Haotian Wang[1], Hongmin Guo[1], Lidong Wang[1,*], Tony D. James[2,3]**

*[1] Hebei Key Lab of Power Plant Flue Gas Multi-Pollutants Control, Department of Environmental Science and Engineering, North China Electric Power University, Baoding, 071003, P. R. China*

*[2] Department of Chemistry, University of Bath, Bath, BA2 7AY, UK*

*[3] School of Chemistry and Chemical Engineering, Henan Normal University, Xinxiang 453007, P. R. China*

# Catalogue

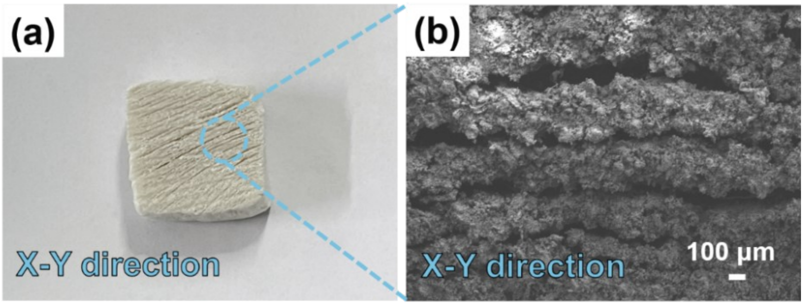

**Fig. S1** Photograph of the wood sponge(a) and its x-y direction SEM images(b).

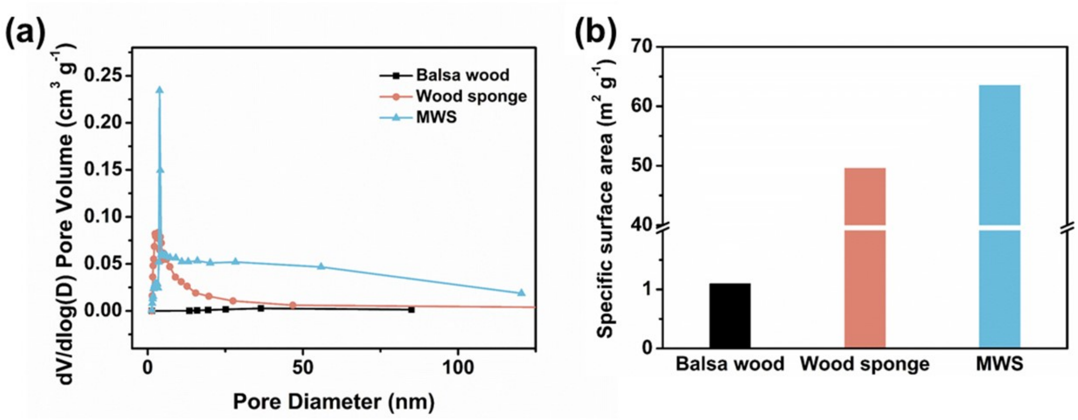


**Fig. S2** (a) Pore size distribution and (b) specific surface area values of balsa wood, wood sponge and MWS.

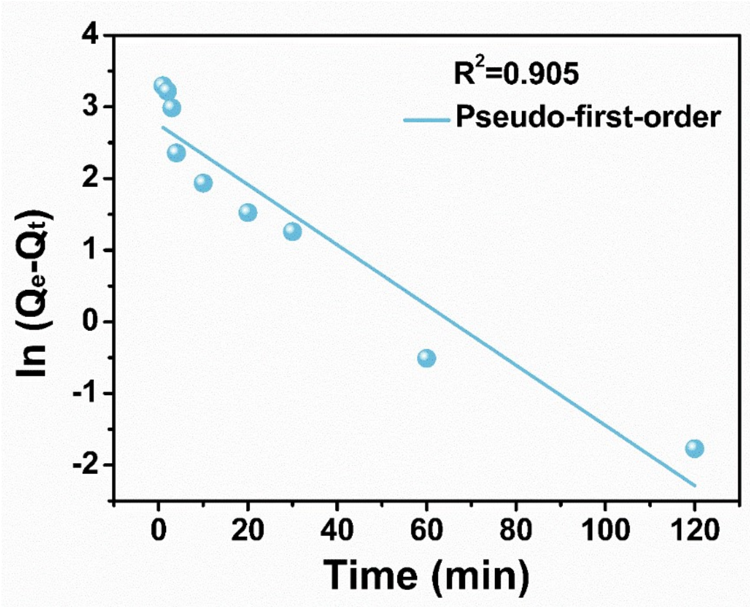


**Fig. S3** Fitting results for pseudo-first-order.

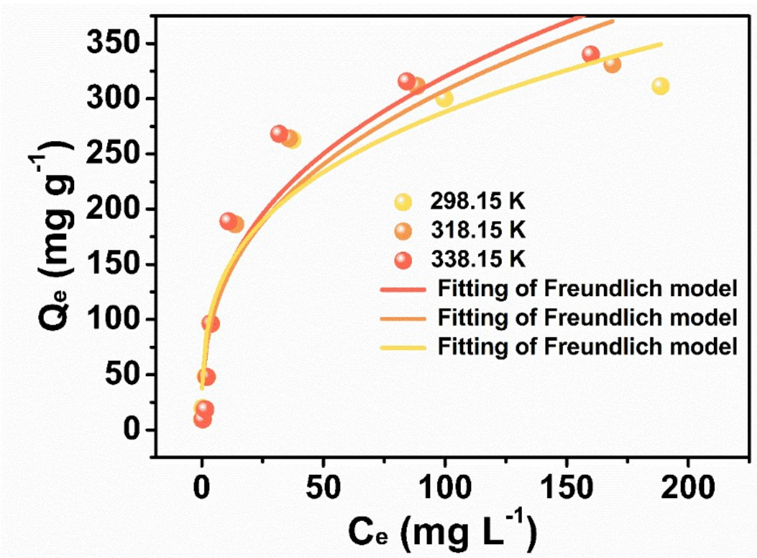


**Fig. S4** Fitting results for Freundlich.

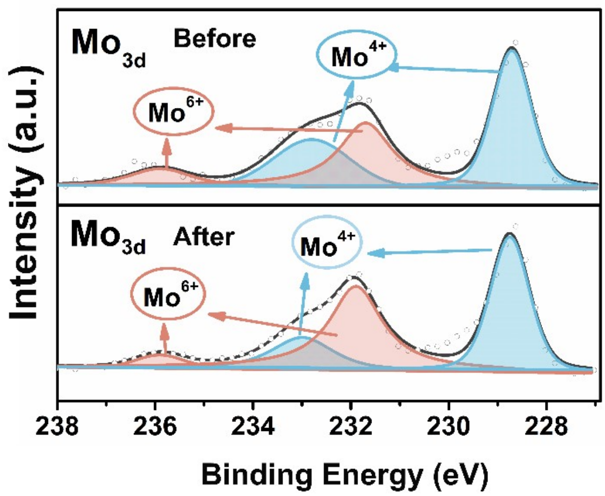


**Fig. S5** XPS spectrum of MWS before and after adsorption of $Hg^{2+}$.

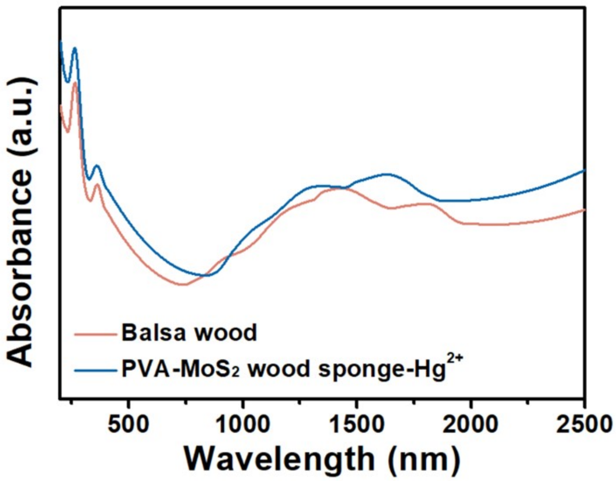


**Fig. S6** UV−Vis−NIR absorption spectra of balsa wood and PVA-MWS-$Hg^{2+}$.

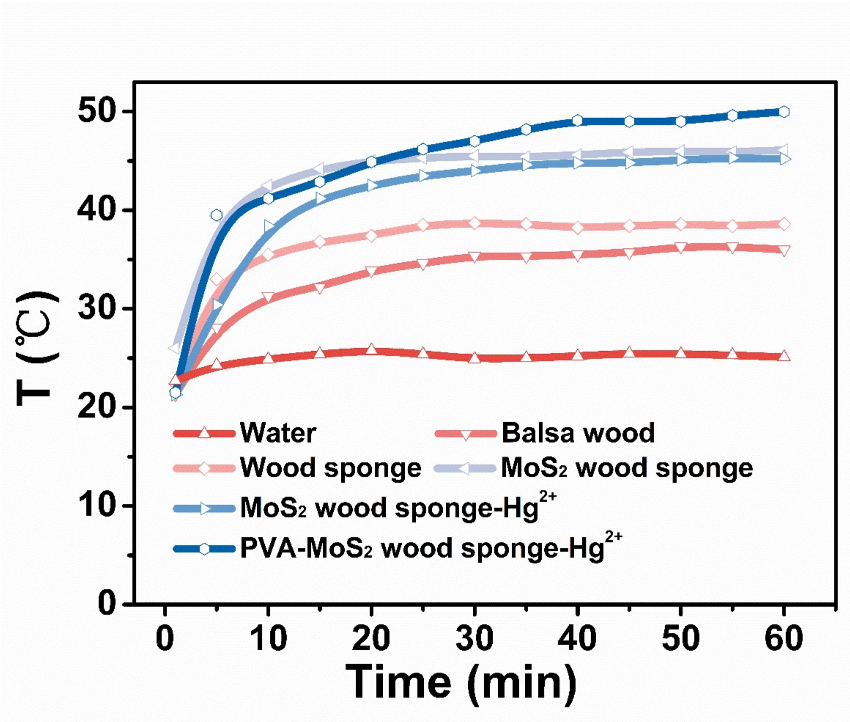


**Fig. S7** The temperature change of different samples under one sun irradiation (100 mW $cm^{-2}$).

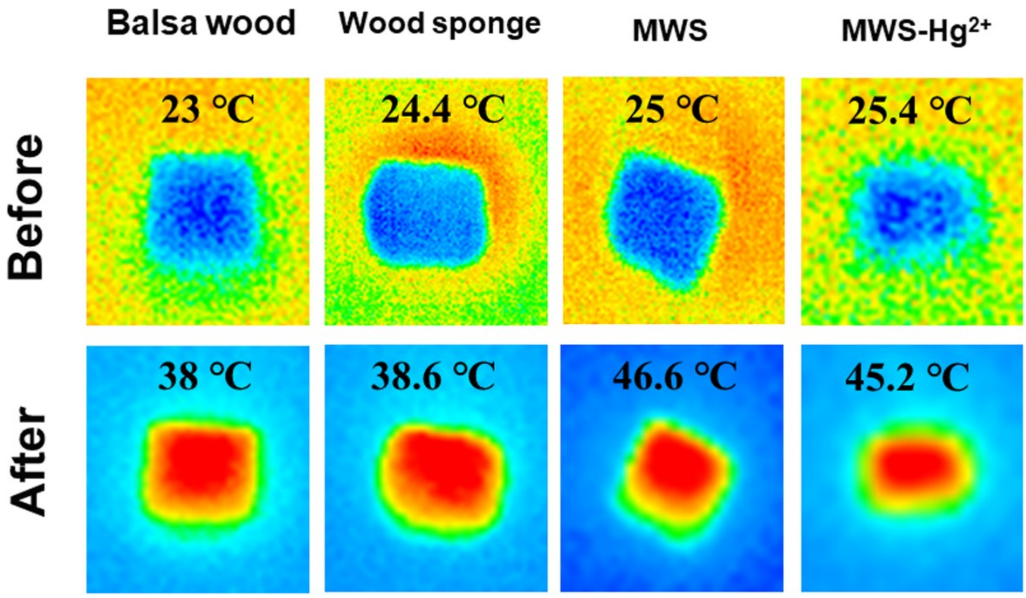


**Fig. S8** Variation of surface temperature at different sample (under 1 sun).

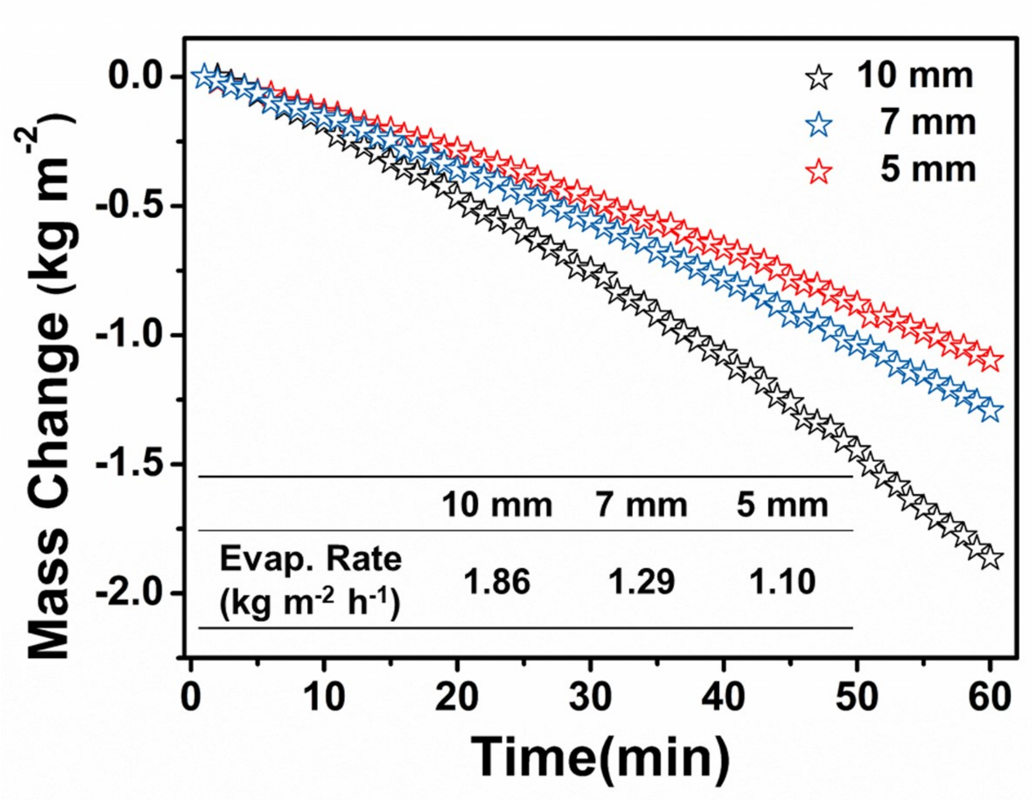


**Fig. S9** Water mass changes with time for PVA-MWS-$Hg^{2+}$ with different substrate thicknesses under 1 $kW \cdot m^{-2}$-simulated light irradiation.

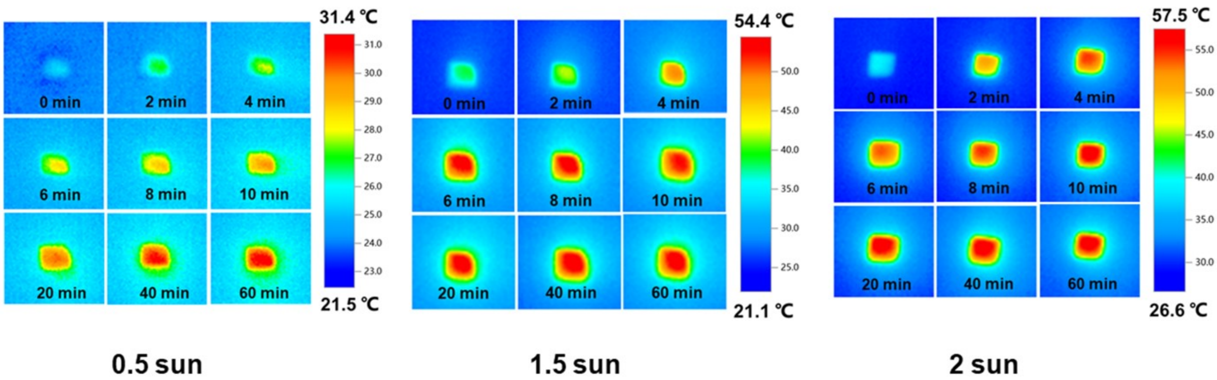


**Fig. S10** Infrared photographs as a function of solar irradiation time for PVA-MWS-$Hg^{2+}$ at different optical concentrations.

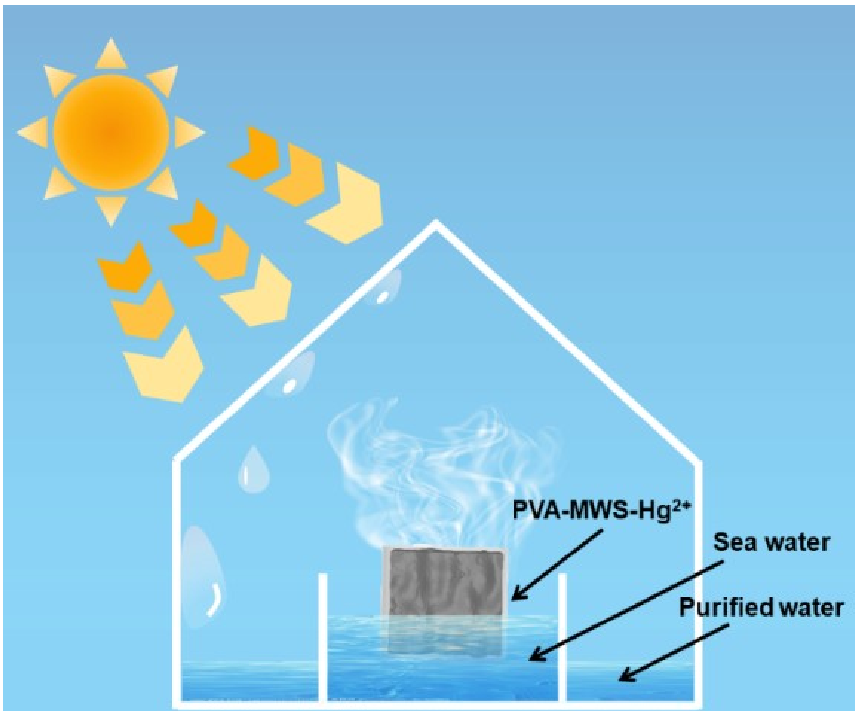


**Fig. S11** Schematic design of the desalination device for water purification.

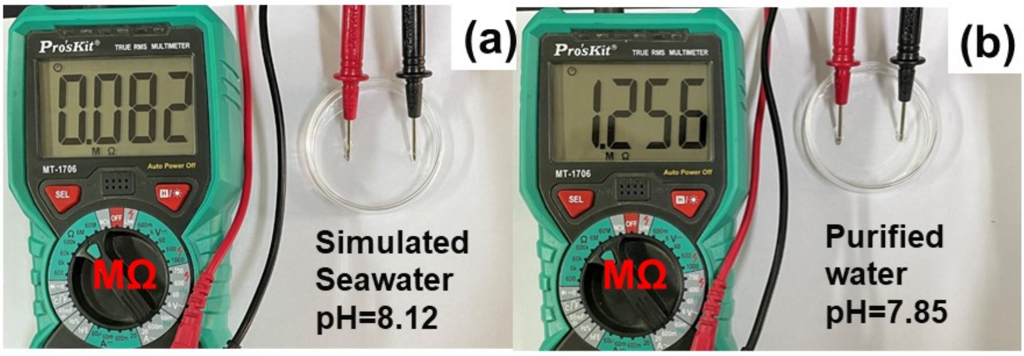


**Fig. S12** Evaluation of water purity using a multimeter with a constant distance between electrodes. (a) Artificial seawater by dissolving salts in deionized water. (b) purified water via the as-developed method.

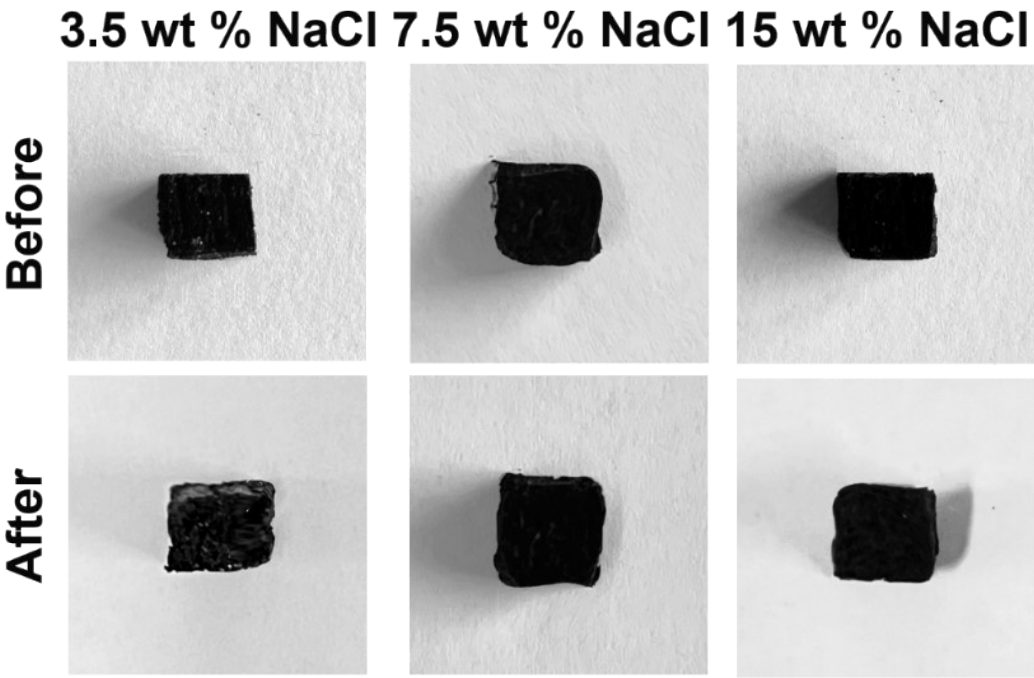


**Fig. S13** The optical images of samples after treatment with different concentrations of NaCl.

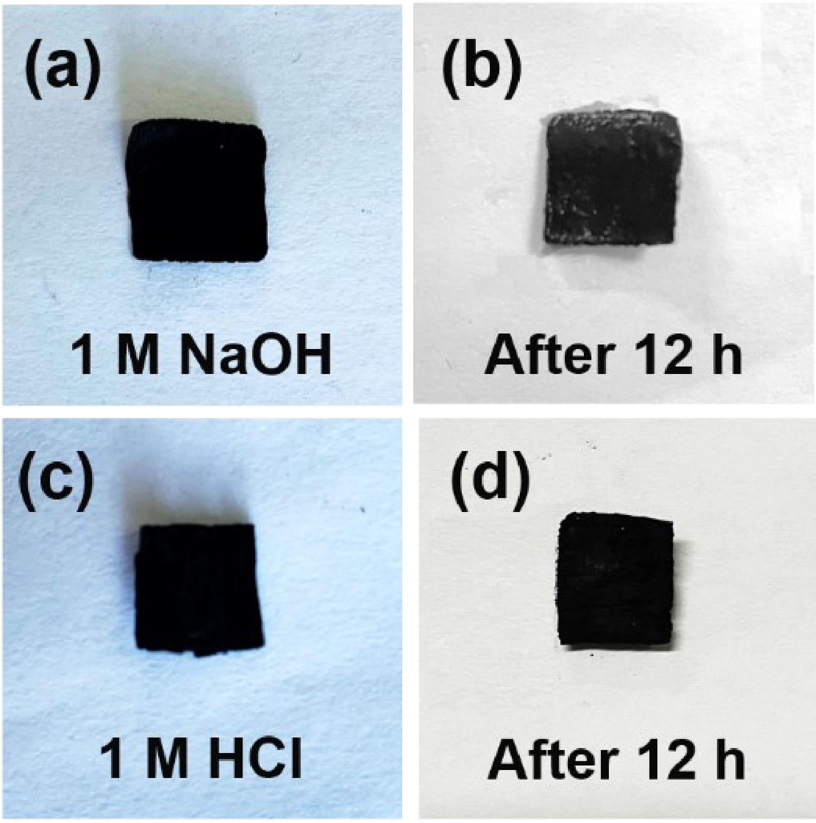


**Fig. S14** The optical images of samples after treatment with (a, b) alkali and (c, d) acids.

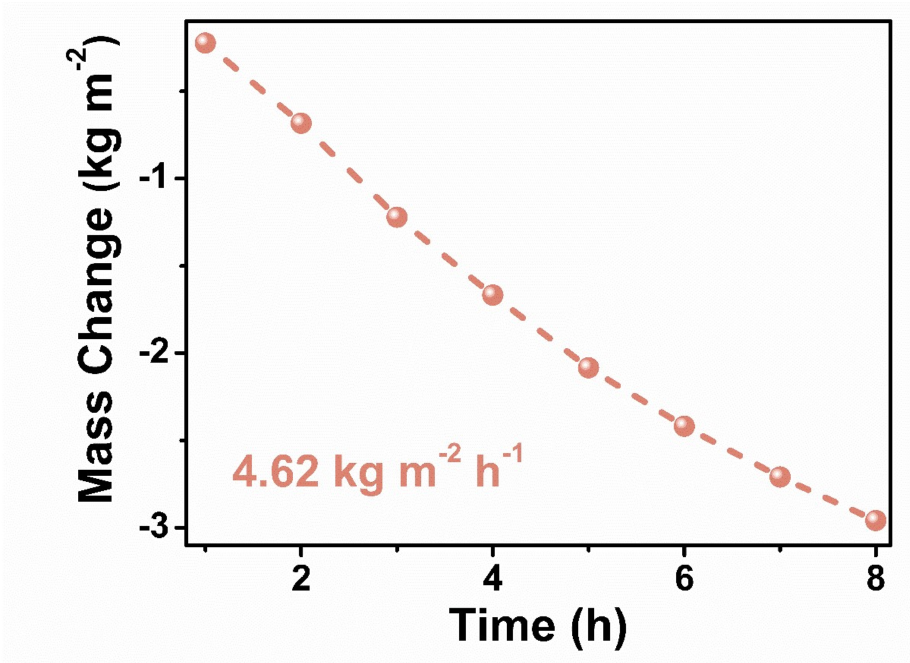


**Fig. S15** Outdoor solar steam generator setup; the mass changes of water for solar steam generation under natural sunlight.

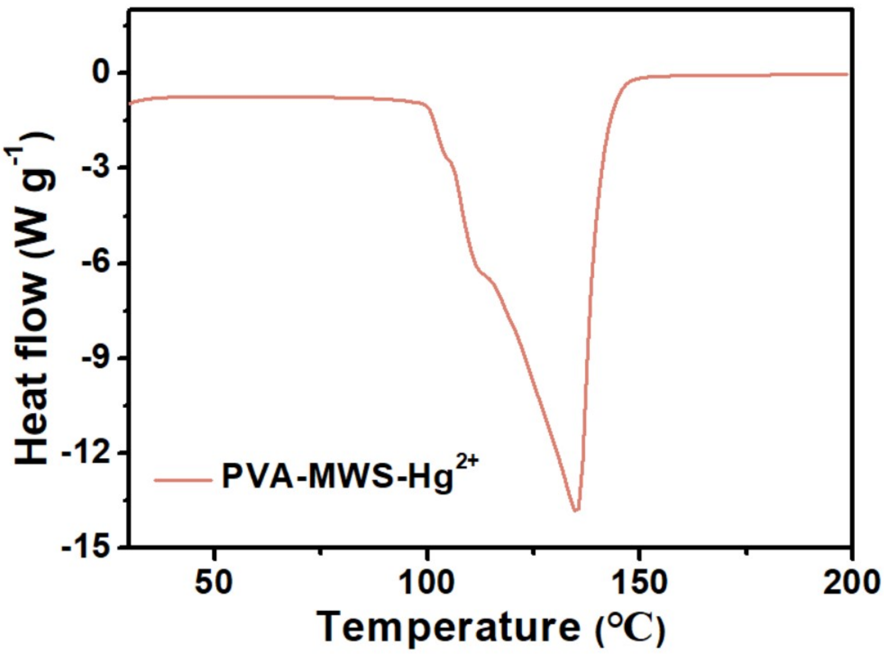


**Fig. S16**. DSC signal of PVA-MWS-$Hg^{2+}$.

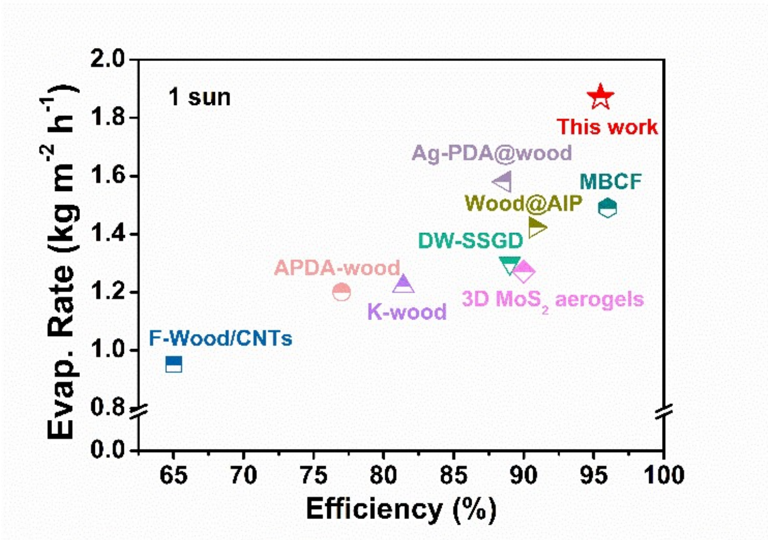


**Fig. S17** Solar steam efficiency compared with the reported evaporation efficiency.

**Table S1** Adsorption parameters of $Hg^{2+}$ ions.

| $C_0$, mg $L^{-1}$ | $q_m$, mg $g^{-1}$ | pseudo-first-order | | | pseudo-second-order | | |
|---|---|---|---|---|---|---|---|
| | | $K_1$, $min^{-1}$ | $q_e$, mg $g^{-1}$ | $R_1^2$ | $K_2$, mg · $g^{-1}$ · $min^{-1}$ | $q_e$, mg $g^{-1}$ | $R_2^2$ |
| 50 | 49.27 | -0.04201 | 15.72 | 0.905 | 0.0111 | 49.776 | 0.999 |

**Table S2** Fitting of adsorption parameters.

| T, K | Langmuir | | | Freundlich | | |
|---|---|---|---|---|---|---|
| | $q_m$, mg $g^{-1}$ | $K_L$, L $mg^{-1}$ | $R^2$ | $K_f$ | n | $R^2$ |
| 298.15 | 325.7329 | 0.1141 | 0.99860 | 71.28447 | 3.29673 | 0.91174 |
| 318.15 | 353.356 | 0.0841 | 0.99627 | 60.10477 | 2.82063 | 0.90916 |
| 338.15 | 362.3184 | 0.0888 | 0.99324 | 62.19228 | 2.81096 | 0.89568 |

**Table S3** Thermodynamic parameters for adsorption of $Hg^{2+}$ on adsorbents.

| $C_0$ | ΔH | ΔS | ΔG (kJ $mol^{-1}$) | | |
|---|---|---|---|---|---|
| mg $L^{-1}$ | kJ $mol^{-1}$ | J $K^{-1}$ $mol^{-1}$ | 298.15 K | 318.15 K | 338.15 K |
| 10 | 56.65 | 284.00 | -28.01 | -33.70 | -39.37 |
| 20 | 46.47 | 247.46 | -27.30 | -32.25 | -37.20 |
| 50 | 12.87 | 129.11 | -25.62 | -28.21 | -30.79 |
| 100 | 9.06 | 114.44 | -25.05 | -27.34 | -29.63 |
| 200 | 8.01 | 107.61 | -24.07 | -26.22 | -28.37 |
| 300 | 6.88 | 98.55 | -22.49 | -24.47 | -26.44 |
| 400 | 6.23 | 87.49 | -19.85 | -22.50 | -23.35 |
| 500 | 6.80 | 84.42 | -18.36 | -20.05 | -21.74 |

**Table S4** Parameters of Langmuir competitive isotherm of $Cd^{2+}$, $Pb^{2+}$ and $Hg^{2+}$.

| Metal | $K_1$ (L $mg^{-1}$) | $K_2$ (L $mg^{-1}$) | $Q_{max}$ (mg $g^{-1}$) | $R^2$ | $Q_{mix}/Q_0$ | MPSD |
|---|---|---|---|---|---|---|
| $Hg^{2+}$(Hg-Pb) | 3.13 | 0.3318 | 364.5 | 0.9377 | 0.9331 | 14.90 |
| $Pb^{2+}$(Hg-Pb) | 2.89 | 0.0701 | 473.3 | 0.9098 | 2.0334 | 17.92 |
| $Hg^{2+}$(Hg-Cd) | 28.62 | 13.4 | 221.8 | 0.9839 | 0.4535 | 15.21 |
| $Cd^{2+}$(Hg-Cd) | 2.94 | 0.7965 | 186.2 | 0.9620 | 1.1909 | 3.09 |

**Table S5** The preparation of simulated desulfurization wastewater.

| Metal | $Hg^{2+}$ | $Cr^{3+}$ | $Cd^{2+}$ | $Pb^{2+}$ | $Cu^{2+}$ |
|---|---|---|---|---|---|
| $C_0$ (ppm) | 0.05 | 1.5 | 0.1 | 1.0 | 1.0 |

**Table S6** The preparation of artificial saline water.

| Water | NaCl | $MgCl_2$ | $MgSO_4$ | $CaSO_4$ | $K_2SO_4$ | $CaCO_3$ |
|---|---|---|---|---|---|---|
| 1000 mL | 27.2 g | 3.8 g | 1.7 g | 1.2 g | 0.1 g | 0.1 g |

**Table S7** Estimation of materials cost for $MoS_2$ wood sponge composite.

| Chemicals | Vendor | Price | | Materials/device | Price/device |
|---|---|---|---|---|---|
| Ammonium molybdate tetrahydrate | Kermel | 500 g | \$ 40.3 | 1.07 g | \$ 0.0856 |
| Thioacetamide | Kermel | 500 g | \$ 22.8 | 0.88 g | \$ 0.0400 |
| Balsa wood | T-mall | 2×2×1 cm | ¥ 0.89 | 2×2×1 cm | \$ 0.1394 |
| Sodium hydroxide | Kermel | 500 g | ¥ 1.25 | 1.33 g | \$ 0.0033 |
| Sodium chlorite | Aladdin | 500 g | \$ 10.962 | 0.33 g | \$ 0.00064 |
| Ethanol | Kermel | 2500 mL | \$ 0.62 | 30 mL | \$ 0.01488 |
| PVA | Kermel | 250 g | \$ 2.346 | 0.167 g | \$ 0.00157 |
| **Cost of $MoS_2$-wood sponge** | | | | | \$ 0.2838 |
| **Cost of PVA-$MoS_2$ wood sponge** | | | | | \$ 0.2854 |